Measurement and assessment of imperfections in plasma cut-welded H-shaped steel columns

P. Arasaratnam[†] and K. S. Sivakumaran[‡]

Centre for Effective Design of Structures, Department of Civil Engineering, McMaster University, Hamilton, Ontario, Canada, L8S 4L7

Kim J. R. Rasmussen[‡†]

Centre for Advanced Structural Engineering, Department of Civil Engineering, The University of Sydney, Sydney, NSW 2006, Australia

Abstract. H-shaped welded steel column members are fabricated by welding together pre-cut flanges and the web. Modern fabricators are increasingly using plasma-cutting technique instead of traditional flame cutting. Different fabrication techniques result in different degrees of geometric imperfections and residual stresses, which can have considerable influence on the strength of steel columns. This paper presents the experimental investigation based temperature profiles, geometric imperfections, and built-in residual stresses in plasma cut-welded H-shaped steel column members and in similar flame cut-welded H-shaped steel columns. Temperature measurements were taken during and immediately after the cutting operations and the welding operations. The geometric imperfections were established at closely spaced grid locations on the original plates, after cutting plates into plate strips, and after welding plate strips into columns. Geometric imperfections associated with plasma cut element and members were found to be less than those of the corresponding elements and members made by flame cutting. The "Method of Section" technique was used to establish the residual stresses in the plate, plate strip, and in the welded columns. Higher residual stress values were observed in flame cut–welded columns. Models for idealized residual stress distributions for plasma cut and flame cut welded sections have been proposed.

Keywords: plasma cutting; flame cutting; plasma cut-welded H-shaped steel columns; experimental; measurements; imperfections; temperature profiles; geometric imperfections; residual stresses.

1. Introduction

H-shaped steel column members may be fabricated by welding together pre-cut flange and web plate strips. Traditional cutting process is by oxygen-acetylene flame, where oxygen gas mix is used to produce a controlled flame at an elevated temperature. This cutting technique is very useful in simultaneous

---

†Graduate Student
‡Professor, Corresponding author, E-mail: siva@mcmaster.ca (This paper was written while the author was a Visiting Professor at the Centre for Advanced Structural Engineering, Department of Civil Engineering, The University of Sydney, Sydney, NSW 2006, Australia)
‡†Professor

multiple-cutting, high production runs at relatively slow speed. Also, this process is an excellent choice for end-users requiring inexpensive cutting through carbon steel and most alloys. Though this method is used to produce near-neat shapes, it creates a large heat affected zone (HAZ) and rough edges that must be removed by additional machining and grinding. With the advancements in manufacturing technologies, however, steel fabricators are using modern cutting techniques such as, plasma cutting, laser cutting, water jet cutting, etc. Plasma (arc) cutting process uses electrically conductive plasma gas jet to cut metals at extremely high temperatures. The cutting process is completed by removing the molten metal with a high velocity jet of ionized gas issued from the constricting orifice. The ability of the process to sever any electrically conductive materials made it highly attractive for cutting nonferrous metals that cannot be cut by the oxy-fuel cutting process. The cutting thickness capability of conventional plasma system varies depending on system manufacturer and power levels. Currently, plasma systems are available to cut aluminium to about 150 mm thick, stainless steel to about 125 mm thick and carbon steels to about 32 mm thick. The quality of the cutting is highly influenced by the hardness of a material to be cut. Plasma cut is faster while producing neat precision cut edges. Plasma cut also produces a heat-affected-zone which is smaller than that caused by a flame cut. As far as the capital cost associated with these cutting systems is concerned plasma cutting system costs are considerably higher than the flame cutting system.

Different fabrication techniques result in different degrees of geometric imperfections. Fabrication methods, which involve heating and cooling to different rate and extent, also induce residual stresses. The initial geometric imperfections and the locked-in residual stresses can have considerable effects on the strength of steel structural members. It has long been established (Huber and Beedle 1954) that these imperfections are dominant in intermediate columns, which are most common in steel buildings. The detrimental effects of imperfections have been incorporated into the current column design provisions given in various national steel design standards. For example, the Canadian Steel Design Standard (CSA 2001) provides two design equations for the design of columns. One for doubly symmetric welded three-plate members with flange edges oxy-flame cut and hollow structural section (Class H - Hot-formed or Cold-formed stress relieved), and another for hot-rolled, fabricated structural sections, and hollow structural sections - Class C - (Cold-formed non-stress relieved). Accordingly, oxy-flame cut-welded sections may carry up to 23% higher axial loads compared to rolled sections. Similarly, the Australian Steel Design standard (SA 1998) provides the following five column design categories recognizing the different imperfections associated with the different fabrication methods.

- Hot-formed hollow sections and cold-formed-stress-relieved hollow sections ($\alpha_b = -1.0$)
- Cold-formed-non-stress relieved hollow sections ($\alpha_b = -0.5$)
- Hot-rolled universal sections (flange thickness up to 40 mm), Welded H and I sections fabricated from flame cut plates, Welded box sections ($\alpha_b = 0.0$)
- Tees flame cut from universal sections and angles, Hot-rolled channels, Welded H and I sections fabricated from as-rolled plates (flange thickness up to 40 mm) ($\alpha_b = +0.5$)
- Hot-rolled universal sections (flange thickness over 40 mm), Welded H and I sections fabricated from as rolled plates (flange thickness over 40mm) ($\alpha_b = +1.0$)

Here, α_b is the compression member section constant established reflecting the imperfections associated with the section. Column members in section category $\alpha_b = -1.0$, depending on the slenderness, can carry up to 52% higher axial loads compared to column members in section category $\alpha_b = +1.0$.

Perhaps due to lack of available data on the geometrical imperfections and residual stress patterns on steel columns fabricated using the plasma cutting techniques current design standards do not include provisions for column members fabricated from plasma cut plates, and the steel designers are concerned

with the use of current code equations to such columns. The primary objective of this part of the investigation is to establish the geometric imperfections and the built-in residual stresses present in plasma cut-welded H-shaped members and in comparable flame cut-welded H-shaped members. The secondary objective is to establish the temperature distribution in such members during these fabrication operations. The temperature distribution results may be of use to validate analytical models of the problem. This paper presents the imperfection characteristics of plasma cut-welded H-shaped steel columns. A large plate was cut into plate strips and then the plate strips (flanges and web) were welded together to form the H-shaped sections used in this investigation. The residual stresses were established at various stages of fabrication processes, using the "method of section" technique. Similarly, the geometrical imperfections were established at various stages of fabrication processes in this investigation. The temperature profiles were measured during and immediately after the cutting and welding processes. This paper presents the temperature profiles, geometric imperfections and residual stresses observed in the test columns. Based on these results residual stress distribution models have been proposed for plasma cut plates, and for columns fabricated from plasma cut plates. It is also of interest to establish the strength of plasma cut-welded H-shaped columns and the strength of comparable flame cut-welded H-shaped columns, however, that part of the investigation is not included in this paper.

2. Investigation methodology and fabrication processes

This section summarizes the research methodology and the fabrication processes used in this investigation. The investigation technique used herein attempts to establish the changes in geometric imperfections and residual stresses as a steel plate is transformed into an H-shaped column member through various fabrication processes. To achieve the objectives of the investigation, the study began with six identical steel plates having the following dimensions; length = 3960 mm, width = 710 mm and thickness = 9.5 mm. These dimensions were determined in consideration of the various tests to be performed and in consideration of the available test facilities. The plates were purchased from a steel wholesaler who assured that all six plates were from the same production batch. The measured yield strength ranged 345-400 MPa (Average yield strength F_y = 374 MPa), whereas the measured ultimate strength of these steel plates ranged 462-472 MPa. Fig. 1 shows the sketch of a whole plate, highlighting the cutting and measurement locations. This investigation consisted of the following major components; (a) preparation of the plates, (b) cutting of the plates into plate strips, (c) welding of flange and web plate strips, (d) measurement of temperature distribution during fabrication, (e) establishment of geometric imperfections, and (f) establishment of residual stresses. Table 1 summarizes the fabrication stages and the measurements associated with this investigation. Further details associated with each of the above components are given in the following sections.

2.1. Stage 1: Preparation of the plates

Immediately after surface cleaning of the six steel plates, the locations of cuts were identified on them. During next stage (stage 2), the plates would be cut along the length direction into flange and web plate strips, thus lines shown as 1-1, 2-2, 3-3, and 4-4 in Fig. 1 were marked on the plates to identify these lines of cut. Note that the flange and web plates were taken from the interior of the plate in order to eliminate the end effects that may exist due to manufacturing and/or previous cutting operations on these plates. The resulting flange and web plate strips are 150 mm wide, and the remnants on either side
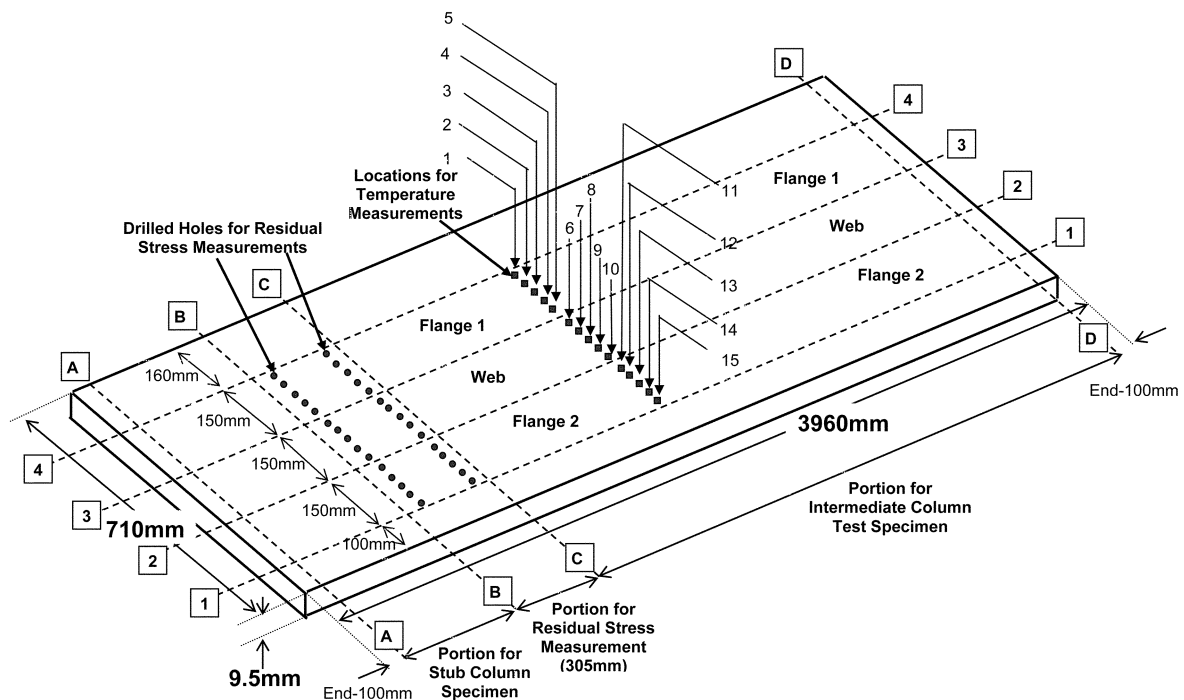
Fig. 1 Identification of fabrication locations and measurement locations in steel plate

of these plates were used to cut out the tension test coupons that were used to establish the mechanical properties of these steel plates. After the flange and the web plates are welded together to form the H-shaped members (stage 3), the long H-shaped members would be transversely saw-cut to obtain a portion for residual stress measurement (stage 4). This portion was about 305 mm long and was cut away from the ends of the member. Lines marked as B-B and C-C, and shown in Fig. 1 signify these transverse lines of cut. The portions on either side of the piece for residual stress measurement form the intermediate column and a stub column test specimens.

Next, the locations for temperature measurements were identified on the original plates. Surface temperatures during fabrication were measured at fifteen locations, consisting of five locations each in flange 1, web, and flange 2, respectively. As identified in Fig. 1, they are equally spaced points (30 mm) located in the middle of the plates. These temperature measurement locations are 20×20 mm squares, painted black in order to obtain an emmisivity of about 1. The 'Method of Section' technique for residual stresses was used in this investigation, which involves water-jet cutting of the member into slices (stage 5). Identification of residual stress measurement locations and drilling of associated holes followed next. Grid lines along the edges of the slices were marked and numbered. Pairs of gauge holes were drilled within each slice using a hand-held drilling machine attached to a drill stand. Further details associated with the temperature, geometric imperfection and of residual stress measurements are provided in the following sections.

2.2. Stage 2: Cutting of the plates

Three plates, designated in this investigation as Plate-01, Plate-03, and Plate-05, were cut by plasma

cutting technique and the other three plates, designated herein as Plate-02, Plate-04, and Plate-06, were cut by the traditional flame cutting operations. The plasma cutting machine operational parameters, and the flame cutting machine operational parameters were selected by the workmen in the fabrication shop based on their own experiences with such fabrications. The workmen were asked to choose the cutting parameters in order to obtain practical results and to avoid external influences in such fabrication processes. The following plasma cutting machine parameters were used to cut Plates-01,-03, and -05; Torch-to-work Distance: 4 mm, Initial Torch Piercing Height: 8 mm, Arc Voltage Setting: 155 Volts, Current: 200 Amps, Travel Speed: 3500 mm/min, Approximate Motion Delay Time: 0.3 sec, Water level: 50 mm below the bottom plate surface. Obviously, these parameters depend on the thickness of the steel plate to be cut, and were selected by the workmen. The observed striking temperature of the plasma-gas during cut was about 650°C. Further, the cutting tolerance associated with plasma-cut plate strips were approximately 1-2 mm, and the cut edges were smooth requiring no further machining. Similarly, the following flame cutting machine parameters were used to cut Plates-02,-04, and -06; Pressure of Oxy Heating Pilot Flame: 2.0 bar, Pressure of Oxy Piercing Flame: 2.0 bar, Pressure of Oxy Heating Cut Flame: 2.0 bar, Heating Height: 4 mm, Piercing Height: 10 mm, Working Height: 18 mm, Piercing Delay: 1.0 sec, Warm Up Time: 25 sec, Cutting Speed: 540 mm/min, Slow down Speed : 400 mm/min. The observed maximum striking temperature for flame cutting was about 850°C. The cutting tolerance associated with flame-cut plate strips were observed to be 2-3 mm and the cut edges were not smooth requiring additional grinding to remove rough edges. Overall, the plasma cutting was faster, while the cut piece experiences lesser striking temperatures. Further, the plasma cut resulted in cuts with better precision and with smoother edges.

2.3. Stage 3: Welding of the flange and web plates

Forming of the H-shaped members was the second part of the fabrication process in this investigation. Automatic Gas Metal Arc (GMAW) welding process with flux core wire and co_2 sealing gas was used to fillet weld the plate strips to form the H-shape. The flange plates and the web plate were joined together by one pass of weld on each side of the web. The welding operation herein was done by automatic equipment moving roughly at a speed of 190 mm/min. Current and voltage used during this process were approximately 330 Amps and 35 Volts, respectively. The selection of current, voltage, welding speed, diameter of wire, etc. depends upon the thickness of the steel plates to be welded, and the local fabricators selected the machine settings for these welding operations. The striking temperature measured during the welding process herein was 1100°C. A total of six 'H' shaped column members were formed.

2.4. Stage 4: Saw-cutting of column members

Immediately after welding the length of the column members was the same as the length of the original plates of 3960 mm. In stage 4, each column member was severed into a specimen for residual stress measurements, a specimen for intermediate column test, and a stub column test specimen, by making transverse cuts along A-A, B-B, C-C, and D-D as shown in Fig. 1. Cold sawing was used for these transverse cuts. The stub columns and the intermediate columns were later subjected to axial loads until failure, however, that part of the investigation is not given in this paper.

2.5. Stage 5: Slicing of the residual stress specimen

The 'method of section' technique used in the residual stress measurements involves further cutting and slicing of the H-shaped portion for residual stress measurements. Water-jet cutting was used for these operations. Further details associated with this stage of fabrication are given in section 5.

2.5.1. Measurements

The temperatures, geometric imperfections and the residual stresses were measured during this investigation. Temperature measurements were taken at the fifteen measurements points indicated in Fig. 1, at certain time intervals during and immediately after the cutting operations and during the welding operations. The measurement procedure, details of the temperature measurement instruments used, and further descriptions associated with temperature measurements and the results are given in section 3. As outlined in Table 1, the geometric imperfection measurements were taken (a) on the original plates, (b) on the flange and web plate strips immediately after the cutting operations, and (c) on the H-shaped welded members immediately after the separation of the long column members into test specimens. Further details associated with geometric imperfections are given in section 4. The "Demec" mechanical dial gauge and the "method of section" technique were used to establish the residual stresses. As outlined in Table 1, the gauge-hole readings, which reflect the residual stresses, were taken (a) on the original plates, (b) on the flange and web plate strips immediately after the cutting operations, (c) on the H-shaped members, immediately after welding, and (d) after slicing of the member. These measurements provided the residual stress changes during different stages of fabrication. Further

Table 1 Fabrication processes and the measurements

Fabrication process	Measurements
Stage 1: Preparation of the plates • Total of six plates	During Fabrication: After Fabrication: • Geometric Imperfection • Residual Stress
Stage 2: Cutting of the plates into strips • Three plates – Plasma-cut • Three plates – Flame-cut	During Fabrication: • Temperature Distribution After Fabrication: • Geometric Imperfection • Residual Stress
Stage 3: Welding of flange and web plate strips • Total of six members	During Fabrication: • Temperature Distribution After Fabrication: • Residual Stress
Stage 4: Saw-cutting of column members • Six Residual Stress Specimens • Six Stub Columns • Six Intermediate Columns	During Fabrication: After Fabrication: • Geometric Imperfection
Stage 5: Slicing of the residual stress specimens (water jet cutting) • Total of Six Specimens (Three Plasma cut – Welded, and Three Flame cut – Welded H-shaped specimens)	During Fabrication: After Fabrication: • Residual Stress

details associated with the residual stress measurements, the residual stress results, and proposals for idealized residual stress patterns on such members are given in section 5.

3. Temperature profiles

Cut and welded steel members, such as the plasma cut-welded and flame cut-welded H-shaped members, are subjected to enormous amount of heat during cutting and welding operations. These operations can cause considerable thermo-elastic-plastic deformations and non-homogenous mechanical characteristics over the cross-section, which can lead to geometric imperfections and build up of residual stresses in such members. Analytical methods, including finite element methods, may be used to predict these imperfections. As evident from recent publications (Potdar and Zehnder 2003, Lindgren 2001a, b, c), considerable progress had been made on finite element method based simulations of complex fabrication processes. Due to the intricate nature of such simulations, which may involve a large number of input parameters, questions related to the choice of parameters and questions related to the accuracy of results may only be resolved by comparing such calculations to experimental results. In this study, experimental establishment of temperatures during fabrication was deemed useful, because such data may then be used to validate analytical results.

Temperature measurements were taken at fifteen locations indicated in Fig. 1, during and immediately after cutting of the plates, as well as during and after the welding process. The Infrared Thermometer [Model # : OS542, Measurements Range: -20°C to 500°C, Response Time: 0.5 sec, Accuracy: ± 2°C of Reading, Emmisivity: 0.98(fixed)] was used to measure low temperature ranges, whereas, the Infrared Pyrometer [Model #: OS3707, Measurements Range: 250°C to 2000°C, Response Time: 0.5 sec, Accuracy: ± 0.40% of Reading, Emmisivity Range: 0.1 to 1.00 in 0.01 Steps (digitally set)] was used to measure high temperatures. As shown in Fig. 1, the surface temperatures during fabrication were measured at five locations each in flange 1, web, and flange 2, respectively. These are equally spaced 20×20 mm squares painted black in order to obtain an emmisivity of about 1 needed for the instruments. Initial temperature measurements were taken prior to these operations, and the temperature measurements were continuously taken until the plate pieces cooled down to ambient temperatures.

3.1. Plasma cutting and flame cutting processes

Three plates, designated in this investigation as Plate-01, Plate-03, and Plate-05, were cut by plasma cutting technique and the other three plates, designated herein as Plate-02, Plate-04, and Plate-06, were cut by the traditional flame cutting operations. The first cut was made along line 1-1, followed by cuts along lines 2-2, 3-3, and 4-4, respectively. In general, the interval for temperature measurements for plasma cutting was two minutes in the beginning and five minutes after cutting. For flame cutting, the initial temperature measurement interval was chosen depending on the speed of the cutting and the time delay between two successive cuttings. However, during cooling period the temperature measurements were taken for every five minutes.

The magnitude of the temperature at a specific location depends on the proximity of the location to the line of cut, and on the time after cutting. Cutting sequence also influences the temperatures at a location. The measurement points 1 to 5 are in Flange 2, and similarly the measurement points 6 to 10, and 11 to 15, are in the web and Flange 2 plates strips, respectively. Thus, cut 1-1 passes adjacent to point 15, cut 2-2 passes between points 10 and 11, cut 3-3 passes between points 5 and 6, and cut 4-4
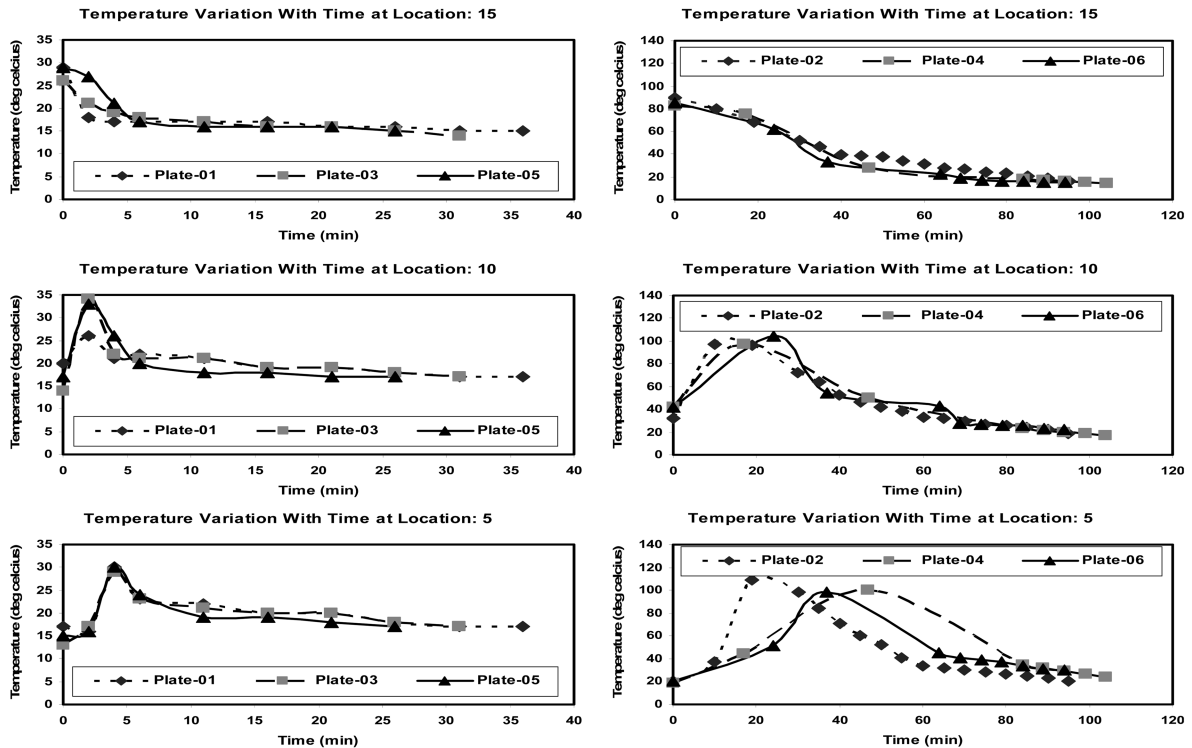
Fig. 2 Temperature variations at locations 15, 10, and 5 in plasma cut plates and in flame cut plates

passes adjacent to point 1. Because of the cutting sequence, a cut along line 1-1 would influence the temperatures at all points, whereas, the cut along line 3-3 will not influence the temperatures at points 10 to 15, since by the time the cut 3-3 is made the plate strip having the points 10 to 15 would have been separated from the larger plate.

Fig. 2 shows the variation of temperature at locations 15, 10 and 5, for Plates -01, -03, and -05 which were plasma cut, and for Plates -02, -04, and -06 which were flame cut. As expected, there is a sudden rise in temperature at point 15, which occurs as soon cut 1-1 is made, then it continuously cools down to ambient temperature. Similarly, points 10 and 5 experience a sudden surge in temperatures immediately after cut 2-2 and 3-3, respectively. Based on Fig. 2, it can be stated that reasonably consistent results were observed during three identical fabrication operations. Any difference is attributable to variations in cutting parameters such as torch-to-work distance and time lag between successive cuts. During plasma cutting the maximum temperatures measured at points 15, 10, and 5 ranged 26°C-29°C, 26°C-34°C and 29°C-30°C, respectively, whereas during flame cutting the maximum temperatures measured at the corresponding points ranged 83°C-89°C, 97°C-104°C and 98°C-109°C, respectively.

Fig. 3 shows representative temperature profiles at all fifteen points during plasma cut (Plate - 03) and during flame cut (Plate - 02). Separate temperature profiles have been given for Flange 2 [Points 10-15], web [Points 6-10] and for Flange 1 [Points 1-5]. Approximate times of the cuts are also shown in these figures. Immediately after cut 1-1, point 15 experiences the highest temperature and all other points experience lesser temperatures depending on the distance from the cut. Note that cut 2-2 influences the
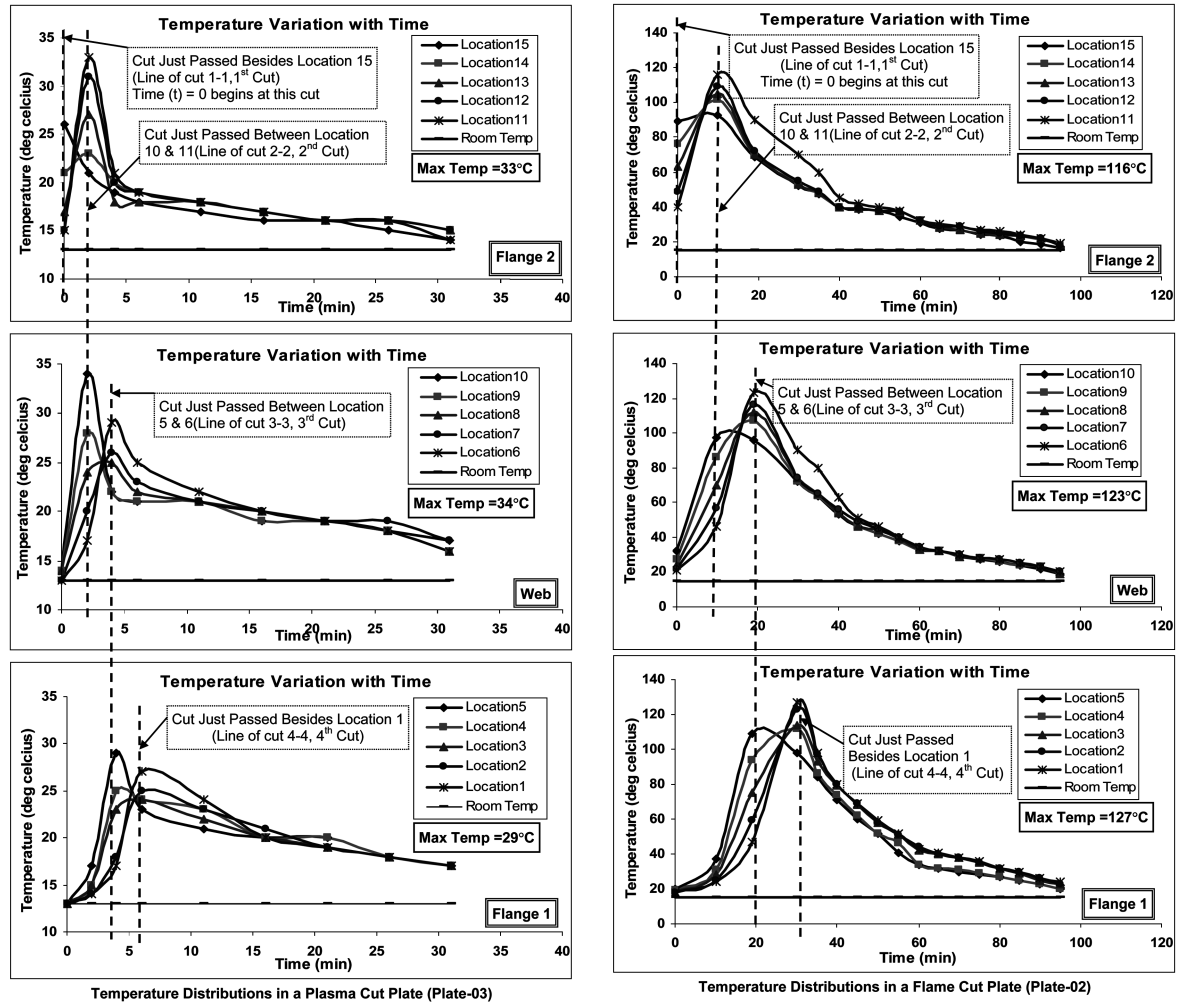
Fig. 3 Temperature distribution in a plasma cut plate and in a flame cut plate

temperatures at points on either side of the cut, therefore the points in Flange 2, and well as points in Web plus Flange 1 segments. However, cut 3-3 influences the temperatures in web and in Flange 1 only, but not the temperatures in Flange 2.

Based on Figs. 2 and 3, and based on other observations and measurements made during this investigation, the following comments can be made. [1] The cutting speed of plasma cutting (3500 mm/min) was more than six times faster than that of flame cutting (540 mm/min). [2] The typical striking temperature measured during plasma cutting was about 650°C, whereas the typical striking temperature measured during flame cutting was about 850°C. [3] The maximum temperature measured in the plate immediately after plasma cutting was 34°C, whereas the maximum temperature after flame cutting was 127°C. [4] Flame cut plates took longer time to cool down to ambient temperatures compared to plasma cut plates. [5] Both cutting methods resulted in somewhat similar general variation of temperature profiles with time.
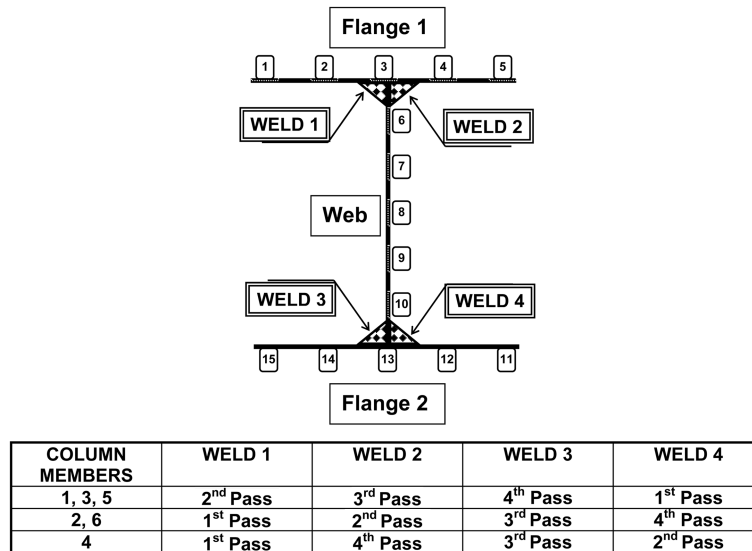
COLUMN MEMBERS	WELD 1	WELD 2	WELD 3	WELD 4
1, 3, 5	2nd Pass	3rd Pass	4th Pass	1st Pass
2, 6	1st Pass	2nd Pass	3rd Pass	4th Pass
4	1st Pass	4th Pass	3rd Pass	2nd Pass

Fig. 4 Sequence of welding for column members

3.2. Welding process

The flange and web plate strips cut from the same original steel plate were welded together to form H-shaped sections. Once again, the fabrication shop workmen determined the weld size and the welding sequence. Nominal leg size of the weld was about 10 mm. The welding sequence included four-passes, where each pass connects the flange plate strips to either side of the web. Fig. 4 provides the weld details. As evident from this figure, the sequence of welding used differed between the column members. Fortunately, however, column members -1, -3, and -5 had the same sequence of welding. During the welding process, the first temperature measurements for each pass were taken as soon as the welding nozzle had just passed the temperature measurements location. Subsequently the temperature measurements were continuously monitored for every five minutes. Figs. 5 and 6 show these measurements, which include the results during the first forty minutes after 1st pass, thirty minutes each after 2nd and 3rd passes, and sixty minutes after 4th weld pass.

Once again, the temperature at a specific location depends on the welding sequence. Fig. 5 shows the temperature variations at locations 8, 13, and 11, which are at the mid-height of the web, flange-web intersection, and the flange tip, respectively. Since all four welds were along the longitudinal edges of the web strip, the temperature variations at location 8 (mid-height of the web) are expected to be somewhat similar regardless of the weld sequence. This is evident in the temperature variations associated with location 8 shown in Fig. 5. Welds 3 and 4 would have significant influence on the temperatures at locations 13 and 11 (locations in flange 2); since these two welds connect the web to flange 2. Considering the temperature results for six column members shown in Fig. 5, as expected, the weld passes associated with welds 3 and 4 cause substantial increases in temperatures at locations 13 and 11. The temperature increase at location 13 is significantly higher than that at location 11 (flange tip). Observing the temperature profiles associated with column members 1, 3 and 5, which had similar weld sequence, it can be concluded that the temperature variations at the same locations for the sections having similar welding sequence were consistent. Though the temperature variation with time is
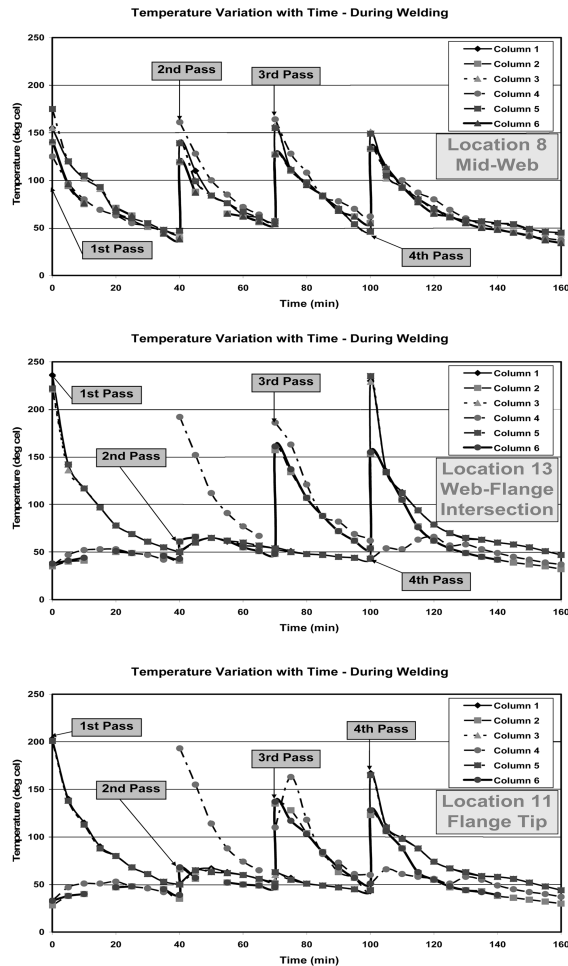
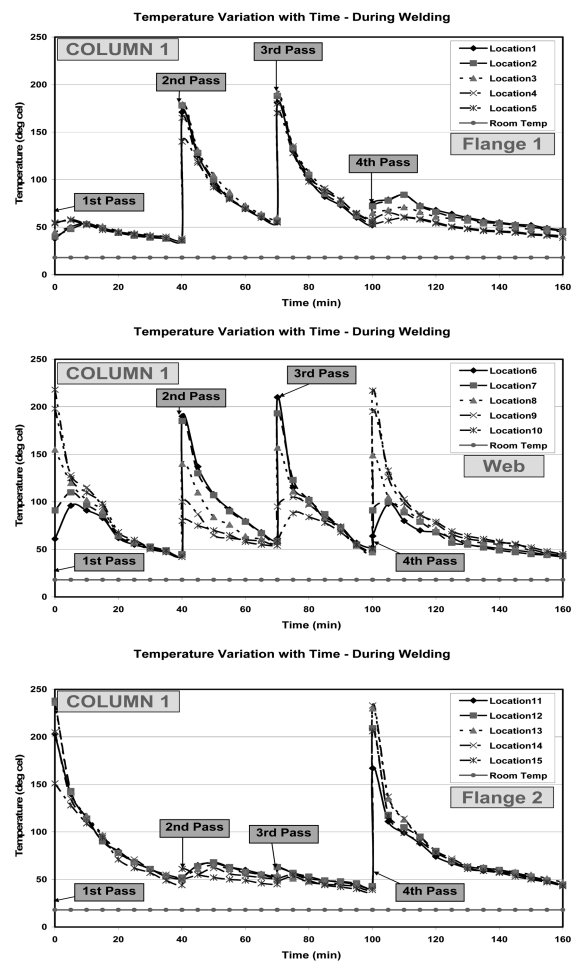Fig. 5 Temperature variations during welding at the mid-web, web-flange intersection, and at the flange tip

Fig. 6 Temperature variations during welding on column member 1

dependent on the weld sequence, the peak temperatures each location experiences seem to be somewhat independent of the weld sequence. A peak temperature of 240°C was recorded in each of the column section. In general, the temperature at flange-web junction was observed to be the highest temperature. A peak temperature of 200°C was noted at the flange tips of column sections 1, 3 and 5. Taking Column section 1 as an example, Fig. 6 shows the representative temperature profiles at all fifteen location during welding. These temperature profiles are obviously associated with the corresponding weld sequence.

4. Geometric imperfections

The geometrical imperfections, such as the out-of-plane deflections in a plate or in plate strips, camber, sweep and variations in sectional dimensions of structural members, can have detrimental effects on the

strength of structural elements and members. The extent of such imperfections in a steel member depends on the fabrication process, cross-sectional size and shape (Nagaraja Rao and Tall 1961), and to a certain degree on the yield strength of steel (Fukumoto and Itoh 1983). However, the permissible initial out-of-straightness, either camber or sweep, and permissible variations in sectional dimensions for different types of sections are limited by the structural steel delivery specifications such as CAN/CSA G40.20 (CISC 2004), and ASTM A6 (ASTM 2004). Often, the permissible variation in initial out-of-straightness is expressed as a fraction of the length of the member. According to CAN/CSA G40.20 (CISC 2004), the permissible variation in straightness for W-shapes specified as columns with flange width approximately equal to width, and welded columns and compression members in truss having a length (L) of less than 14,000 mm, such as the members used in this investigation, is specified as $L/1,000 \le 10$ mm. This tolerance limit applies to camber or sweep. Further, according to CAN/CSA G40.20 standard (CISC 2004) the permissible variations in sectional dimensions for welded shapes are as given in Table 3(a). The geometrical imperfections were established at various stages of the fabrication processes such as [a] the original plates, [b] the plate strips after cutting, and [c] the column members. The sectional variations such as out-of-squareness of sections and out-of-flatness of sectional elements were also observed.

The original steel plates (dimensions: length = 3960 mm, width = 710 mm and thickness = 9.5 mm) were supported on a flat surface, and the out-of-plane imperfections were measured along predetermined gridlines. Along the longitudinal direction, the imperfections were measured at approximately 300 mm intervals along lines; 1-1, 2-2, 3-3, 4-4 (Fig. 1), and along mid-lines between these lines. Thus, measurements were taken along seven longitudinal lines spaced at 75 mm. Geometric imperfections were also measured in the transverse direction along three gridlines located at quarter and half-length of the plate (i.e., lines 990 mm apart). The imperfections were measured along these lines at 100 mm intervals. A string and plumb-bobs at its ends placed along the gridline was used in imperfection measurements. The out-of-plane imperfections were measured using a flat ruler having a least count of 0.5 mm. Table 2(a) summarizes the maximum out-of-plane imperfections measured on six plates before and after cutting. Prior to cutting, the maximum out-of-plane imperfections measured in Plates 01, 03 and 05 were about 2.5 mm (L/1584), 1.5 mm (L/2640), and 3 mm (L/1320), respectively. The

Table 2(a) Measured maximum out-of-plane geometric imperfections in plates and in plate strips

Plate	State	Location		
		Flange 1	Web	Flange 2
Plate – 01 L = 3960 mm	Before Cutting	2.5 mm (L/1584)	2.5 mm (L/1584)	2.5 mm (L/1584)
	After Plasma Cutting	3.0 mm (L/1320)	3.0 mm (L/1320)	3.5 mm (L/1131)
Plate – 02 L = 3960 mm	Before Cutting	13.0 mm (L/305)	11.5 mm (L/344)	11.5 mm (L/344)
	After Flame Cutting	17.0 mm (L/233)	16.0 mm (L/248)	10.0 mm (L/396)
Plate – 03 L = 3960 mm	Before Cutting	1.5 mm (L/2640)	1.5 mm (L/2640)	1.5 mm (L/2640)
	After Plasma Cutting	2.0 mm (L/1980)	1.5 mm (L/2640)	2.5 mm (L/1584)
Plate – 04 L = 3960 mm	Before Cutting	12.5 mm (L/317)	13.0 mm (L/305)	13.0 mm (L/305)
	After Flame Cutting	14.0 mm (L/283)	12.0 mm (L/330)	7.0 mm (L/566)
Plate – 05 L = 3960 mm	Before Cutting	2.5 mm (L/1584)	3.0 mm (L/1320)	2.0 mm (L/1980)
	After Plasma Cutting	3.5 mm (L/1131)	3.0 mm (L/1320)	3.0 mm (L/1320)
Plate – 06 L = 3960 mm	Before Cutting	6.5 mm (L/609)	6.5 mm (L/609)	7.0 mm (L/566)
	After Flame Cutting	9.5 mm (L/417)	9.5 mm (L/417)	9.0 mm (L/440)

Table 2(b) Measured maximum sweep and camber in test column members

Column member	Cutting method	Length	Imperection	
			Sweep	Camber
Column – 1A	Plasma cut-welded	2650 mm	2.0 mm (L/1325)	0.5 mm (L/5300)
Column – 1B	Plasma cut-welded	700 mm	0.0 mm (L/∞)	0.0 mm (L/∞)
Column – 2A	Flame cut-welded	2653 mm	3.0 mm (L/884)	1.0 mm (L/2653)
Column – 2B	Flame cut-welded	696 mm	0.0 mm (L/∞)	0.0 mm (L/∞)
Column – 3A	Plasma cut-welded	2144 mm	2.0 mm (L/1072)	1.0 mm (L/2144)
Column – 3B	Plasma cut-welded	1214 mm	1.0 mm (L/1214)	0.0 mm (L/∞)
Column – 4A	Flame cut-welded	2149 mm	3.0 mm (L/716)	0.5 mm (L/4298)
Column – 4B	Flame cut-welded	1210 mm	0.5 mm (L/2420)	0.0 mm (L/∞)
Column – 5A	Plasma cut-welded	3077 mm	3.0 mm (L/1026)	0.5 mm (L/6154)
Column – 5B	Plasma cut-welded	308 mm	0.0 mm (L/∞)	0.0 mm (L/∞)
Column – 6A	Flame cut-welded	3081 mm	4.5 mm (L/685)	1.5 mm (L/2054)
Column – 6B	Flame cut-welded	306 mm	0.0 mm (L/∞)	0.0 mm (L/∞)

corresponding geometric imperfections for Plates 02, 04, and 06 were 13.0 mm (L/305), 13.0 mm (L/305), and 7.0 mm (L/566), respectively. For no apparent reason, these imperfections happened to be larger than those measured on Plates -01, -03 and -05. As a ratio of the length, the largest out-of-plane imperfection measured in the six plates under consideration was (L/305).

   The out-of-plane imperfections were also measured on the plate strips (3960×150×9.5 mm) after each of the original steel plates was cut into two flange pieces and a web piece. Again, the geometrical imperfections along the longitudinal direction were taken at approximately 300 mm intervals along the lines; 1-1, 2-2, 3-3, 4-4 (Fig. 1), and along mid-lines between these lines. Thus, measurements were taken along seven longitudinal lines spaced at 75 mm. However, no measurements were taken in the transverse direction of the plate strips since no significant imperfections exist in that direction. As shown in Table 2(a), the maximum out-of-plane imperfections in the plate strips cut from Plates 01, 03, and 05, which were plasma cut, were 3.5 mm (L/1131), 2.5 mm (L/1584), and 3.5 mm (L/1131), respectively. The maximum out-of-plane imperfections measured in plate strips cut from Plates 02, 04, and 06, which were flame cut, were 17.0 mm (L/233), 14.0 mm (L/283), and 9.5 mm (L/417), respectively. It was observed that the plate strips cut by oxy-acetylene flame exhibited significant changes in the out-of-plane imperfections than those of the plate strips obtained by a plasma cut. As a ratio of the length, the largest out-of-plane imperfection measured in the plate strips was (L/233).

   The stage 3 involved welding of the flange and web plates resulting in six 3960 mm long H-shaped members. In stage 4, each column member was severed, by making transverse cuts along A-A, B-B, C-C, and D-D as shown in Fig. 1, into a specimen for residual stress measurements, a specimen for intermediate column test, and a stub column test specimen. This investigation therefore involved twelve test column specimens, which are identified in Table 2(b) as column 1A through to 6B. The shortest column member was 306 mm long, whereas the longest column member was 3081 mm long. The sweep, which is the in-plane imperfection of the flange plates (producing minor-axis imperfections), and the camber, which is the in-plane imperfection of the web (producing major-axis imperfections), were measured in the column members by extending strings between the ends and measuring the deviations from straightness at regular intervals. The measurement interval, however, depended on the length of the column member under consideration and varied between 50 mm and 265 mm. The sweep
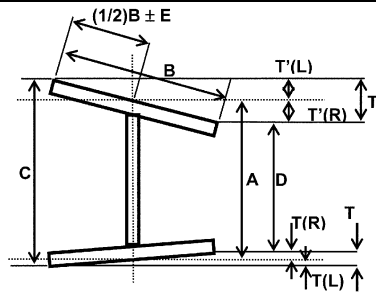
Table 3(a) Permissible variations in sectional dimensions of welded structural shapes having nominal depth of 900 mm and under (CISC 2004)

Depth A, mm	Over	5 mm
	Under	3 mm
Out of parallel (C – D) mm [See Note 1]	N/A	N/A
Width of flange B, mm	Over	6 mm
	Under	5 mm
Web off-centre E, mm	Maximum	6 mm
Combined warpage and tilt, T(L), T(R), T'(L) or T'(R) mm [See Note 2]	Maximum	Greater of B/100 or 6 mm
Out of square, (T + T') mm [See Note 1]	N/A	N/A
Web flatness [See Note 2]	Maximum	A/150 mm

Note 1. N/A – Not available
Note 2. The combined warpage and tilt of the flange is measured from the toe of the flange to a line normal to the plane of the web through the intersection of the centreline of the web with the outside surface of the flange plate.
Note 3. The deviation from flatness of the web is measured in any length of the web equal to the total depth of the beam.

of a column member was measured on the top-flange, on the bottom-flange, and at the mid-height of the web. When measuring the sweep of flanges, first a string was placed along the edges of flange in a closed loop, using flange tips as anchor points. The string was then firmly tightened and held by a turn buckle, when the measurements were taken using a flat ruler having a least count of 0.5 mm. The sweep of the web was measured by looping the string at the web mid-height. Similar procedure was followed in measuring the camber of a column member, however, the string was close looped around the opposite flange-web junctions. Table 2(b) shows the measured maximum sweep and the camber in the test column members under consideration. The largest sweep and camber seemed to occur in the vicinity of the mid length of specimens. A largest sweep of 4.5 mm was observed in the 3081 mm long test column, which translates into a sweep of L/685, where L is the length of the corresponding member. A largest camber of 1.5 mm was measured on the 3081 mm long column member, which represents a camber of L/2054. The largest camber and sweep as presented in Table 2(b) were compared against the permissible variations in straightness (L/1,000 ≤ 10 mm) and it is evident that the camber associated with all twelve column members was within the tolerance, and the sweep associated with column members 2A, 4A, and 6A, however, exceeded the tolerance limits.

　As indicated, the column members under consideration were to be fabricated from 150 mm wide 9.5 mm thick plate strips. Thus, the specified dimensions of the column sections are; flange width 150 mm, flange thickness 9.5 mm, depth 169 mm, and web thickness 9.5 mm. However, in order to

Table 3(b) Measured sectional dimensions of the column members (Specified depth=169 mm, specified width of flange = 150 mm)

		Permissible Depth		Permissible Width		Permissible Web Off-Centre	Permissible Combined Warpage and Tilt		Permissible Web Flatness
		166 mm < A < 174 mm $(169-3$ mm$) < A$ $< (169 + 5$ mm$)$		145 mm < B < 156 mm $(150-5$ mm$) < A$ $< (150 + 6$ mm$)$		Maximum 6 mm	Maximum greater of $(150/100)$ mm or 6 mm. Thus, maximum 6 mm		Maximum 169/150 mm = 1.1 mm
Column Member	Cutting Method	Measured Depth A	Out of Parallel (C − D)	Measured Width B		Measured Web off Centre E	Measured Combined Warpage and Tilt T'(L), T'(R), T(L) or T(R)	Out of Square T'+T	Web Flatness
Column −1	Plasma Cut-Welded	163 mm $(169-6$ mm$)$	4 mm	Top Flange	148mm $(150-2$ mm$)$	± 0.0 mm	0.5 mm and 1.0 mm	4 mm	0.32 mm
				Bottom Flange	148mm $(150-2$ mm$)$	± 1.0 mm	1.5 mm and 1.0 mm		
Column −2	Flame Cut-Welded	167 mm $(169-2$ mm$)$	9 mm	Top Flange	146mm $(150-4$ mm$)$	± 1.0 mm	2.0 mm and 2.0 mm	9 mm	0.64 mm
				Bottom Flange	149mm $(150-1$ mm$)$	± 0.5 mm	1.0 mm and 4.0 mm		
Column −3	Plasma Cut-Welded	167 mm $(169-2$ mm$)$	2 mm	Top Flange	154mm $(150+4$ mm$)$	± 2.0 mm	0.0 mm and 1.0 mm	2 mm	0.79 mm
				Bottom Flange	146mm $(150-4$ mm$)$	± 1.0 mm	0.0 mm and 1.0 mm		
Column −4	Flame Cut-Welded	171 mm $(169+2$ mm$)$	1 mm	Top Flange	145mm $(150-5$ mm$)$	± 0.5 mm	3.0 mm and 1.0 mm	7 mm	0.79 mm
				Bottom Flange	150mm $(150-0$ mm$)$	± 2.0 mm	1.0 mm and 2.0 mm		
Column −5	Plasma Cut-Welded	166mm $(169-3$ mm$)$	5 mm	Top Flange	146mm $(150-4$ mm$)$	± 0.0 mm	0.5 mm and 1.5 mm	5 mm	0.77 mm
				Bottom Flange	147mm $(150-3$ mm$)$	± 0.5 mm	0.5 mm and 2.5 mm		
Column −6	Flame Cut-Welded	166mm $(169-3$ mm$)$	7 mm	Top Flange	149mm $(150-1$ mm$)$	± 3.5 mm	0.0 mm and 1.0 mm	7 mm	0.77 mm
				Bottom Flange	149mm $(150-1$ mm$)$	± 0.5 mm	1.0 mm and 5.0 mm		

establish the variations in sectional dimensions, representative cross-sectional shape of the column members were established. Fig. 7 shows the trace of the cross-section of the six column members, which were taken at one end of the portion for residual stress measurement (see Fig. 1). The plasma cut-welded sections and the flame cut-welded sections have been grouped together and their webs have been vertically aligned, so that the out-of-squareness and the out-of parallel may be visible in Fig. 7. The web depth A, flange width B, and other pertinent dimensions shown in Fig. 7 were measured from
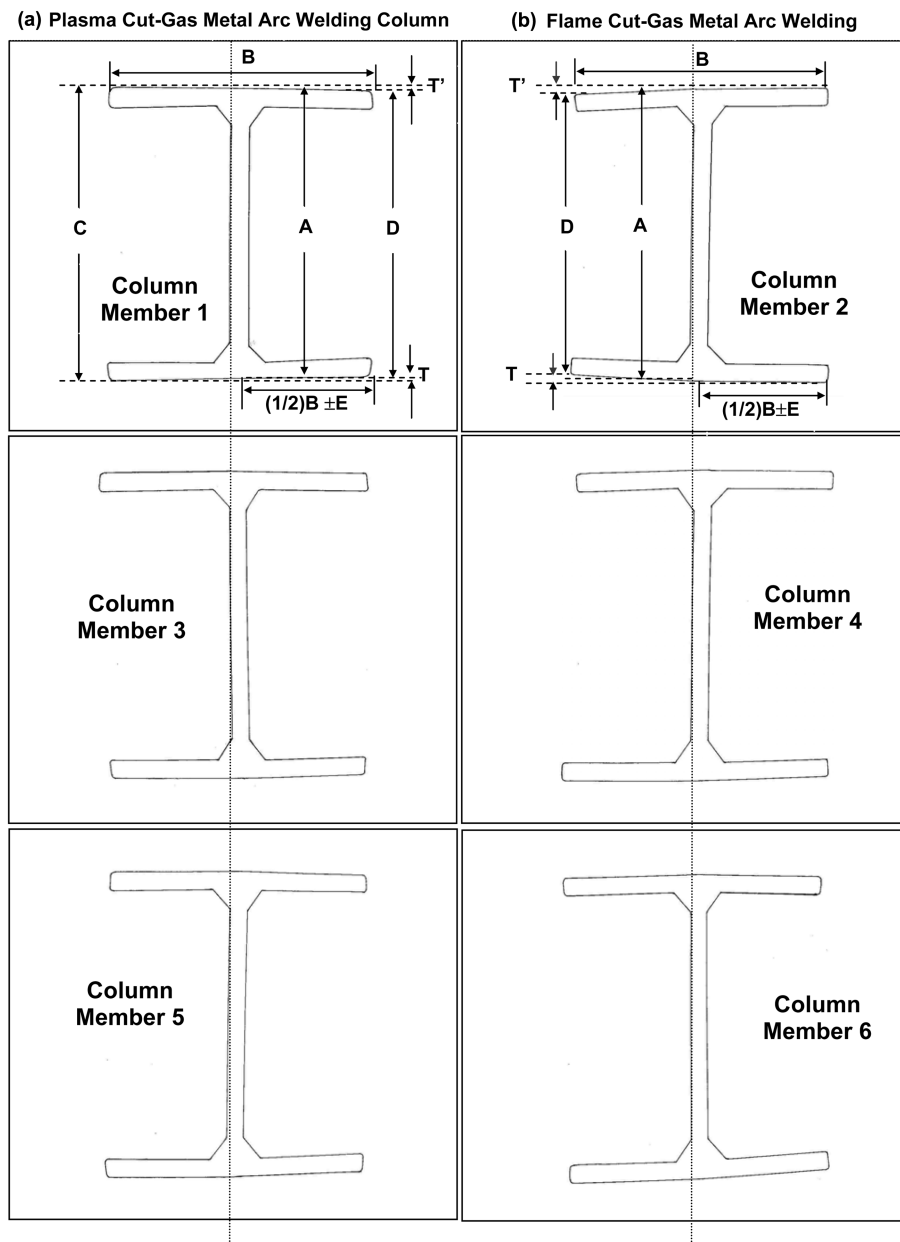

Fig. 7 Variations in sectional dimensions on column members

these traces. From these measurements out-of parallel (C-D), web off-centreline (E), combined warpage and tilt of the flanges (T and T'), out-of-squareness (T+T'), and web flatness were established, which were then compared with the permissible variations in sectional dimensions as provided in CAN/CSA G40.20 (CISC 2004). Table 3(a) shows the permissible variations in sectional dimensions for welded shapes, whereas Table 3(b) shows the measured and derived parameters for the column members. The CAN/CSA G40.20 (CISC 2004) stipulates permissible variations in section depth, width of flanges, combined warpage and tilt, web off-centre and web flatness for welded shapes, however, for wide-flange shapes it stipulates permissible variations in section depth, width of flanges, out-of-squareness, out-of-parallel, web off-centreline, and maximum overall depth at any cross-section. Table 3(a) lists the permissible variations for welded structural shapes such as the column members under consideration, however, the Table 3(b) provides additional relevant information. Except for column 1, the depth of the column members were within the permissible depth range, though the majority of column depths were under the specified depth of 169 mm. The variations in width of flange (B) and the variations in web off-centerline (E) were within the code limits. Table 3(b) shows the combined warpage and tilt for top flange and for bottom flange. The values for left flange toe and for right flange toe have been given separately. It is evident from the measurements given in Table 3(b), the combined warpage and tilt, and the web flatness of all column members were well within the corresponding permissible values. Out of parallel in the column sections ranged between 1 mm and 9 mm, and the out of squareness in the column members ranged between 2 mm and 9 mm. The cross-sections of column members 2, 4 and 6, which were fabricated from flame cut plate strips, exhibited larger out of parallel and out of squareness.

5. Residual stresses

The residual stresses are the built-in stresses in a structural member prior to application of external loads or temperature gradients. These stresses primarily arise due to uneven heating and cooling associated with the fabrication processes, thus, the magnitude and the distribution of residual stress largely depend on the method used in manufacture of the steel member. It has long been established (Huber and Beedle 1954) that the strength of column member is related to residual stresses; therefore, the fabrication process has a direct bearing on the strength of a column member. This part of the investigation experimentally establishes the residual stresses present in a plasma cut-weld column member and in a flame cut-welded column member. A number of residual stress measurement techniques exist, which can be broadly classified as non-destructive, semi-destructive and fully-destructive methods. Diffraction based methods such as X-ray diffraction, synchrotron, neutron diffraction are widely used non-destructive techniques (Kandil *et al.* 2001). The diffraction methods rely on the detection of elastic deformations within a polycrystalline material to establish the internal residual stresses. Though the diffraction methods can provide three dimensional strains mapping of a structural member, at relatively higher costs compared to other techniques, such detailed strain/stress measurements are not warranted for the present investigation. One of the widely used semi-destructive techniques for measuring residual stresses is the hole-drilling strain gauge method. The basic idea involves drilling of a small hole into the member, and subsequent measurement of relieved surface strains using strain rosettes. In this investigation, however, a fully-destructive technique called the "method of section" was used to establish the residual stress distributions in plates, plate strips and in column members. The "method of section" technique was selected for its versatility and cost effectiveness. This technique is well suited for measuring of residual stresses in the longitudinal direction, assuming that the transverse stresses are
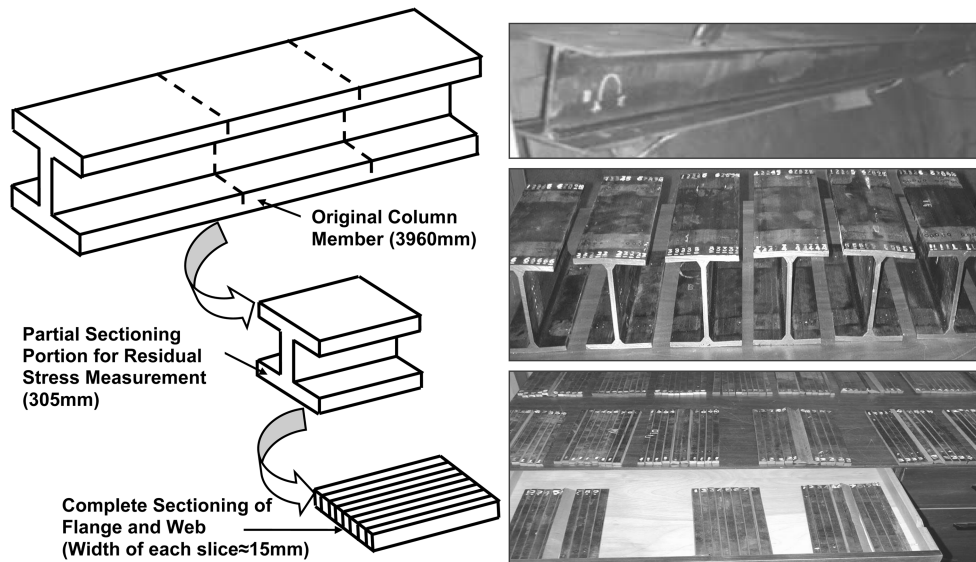
Fig. 8 The 'Method of Section' technique for residual stress measurement

negligible and the slicing process itself produces no appreciable strains. The basic steps associated with the sectioning method are fully described in Guide to Stability Design Criteria for Metal Structures (Galambos 1988) and are summarized in Fig. 8. In the first step, a specimen on which residual stress measurements are to be taken is cut from an original steel section (stage 4). In this investigation 305 mm long sections were cold-sawn from each of the six column members. In the next step the flanges and the web were sliced into 15 mm strips, using a water-jet cutting machine. Water-jet cutting technique is faster and imparts no heat into the work piece. The residual stress measurements were taken on three plasma cut-welded H-shaped columns, and three flame cut-welded H-shaped columns. Fig. 8 also shows the photographic images of the actual specimens after partial sectioning, and after complete sectioning. The state of strain in the 15 mm slices were taken as the reference strain of zero. If the strains were measured before and after slicing, then the change in strain indicates the residual strain, which when multiplied by the modulus of elasticity of steel (200,000 MPa) gives the residual stress.

Based on the observations and experiences gained during this investigation, here we provide some additional points associated with the "Method of Section" residual stress measurement technique. Pilot tests established that use of a mechanical extensometer 'Demec Gauge' or an electrical strain gauge results in identical strain measurements (Arasaratnam 2005). Though, mechanical extensometer is versatile and provides inexpensive strain measurements, the accuracy of the strain measurements depends on the precision and cleanliness of the gauge holes used. Pilot tests established that #55 drill bit produces the best matching gauge holes for the extensometer used in this investigation. It is essential that the gauge holes be drilled perfectly normal to the test surface, which was achieved by the use of a hand-drill machine connected to a drill-stand. Earlier studies established that since the surface strains are measured by this method, the "method of section' technique required an assumption that the residual stresses are uniformly distributed through the thickness, which is appeared to be valid for plate thicknesses less that 37 mm (Nagaraja Rao and Tall 1961). This assumption was verified correct during pilot tests, when the strain measurements taken on opposite faces of a plate element were found to be almost equal to each other (Arasaratnam 2005). In this investigation, each gauge hole was drilled
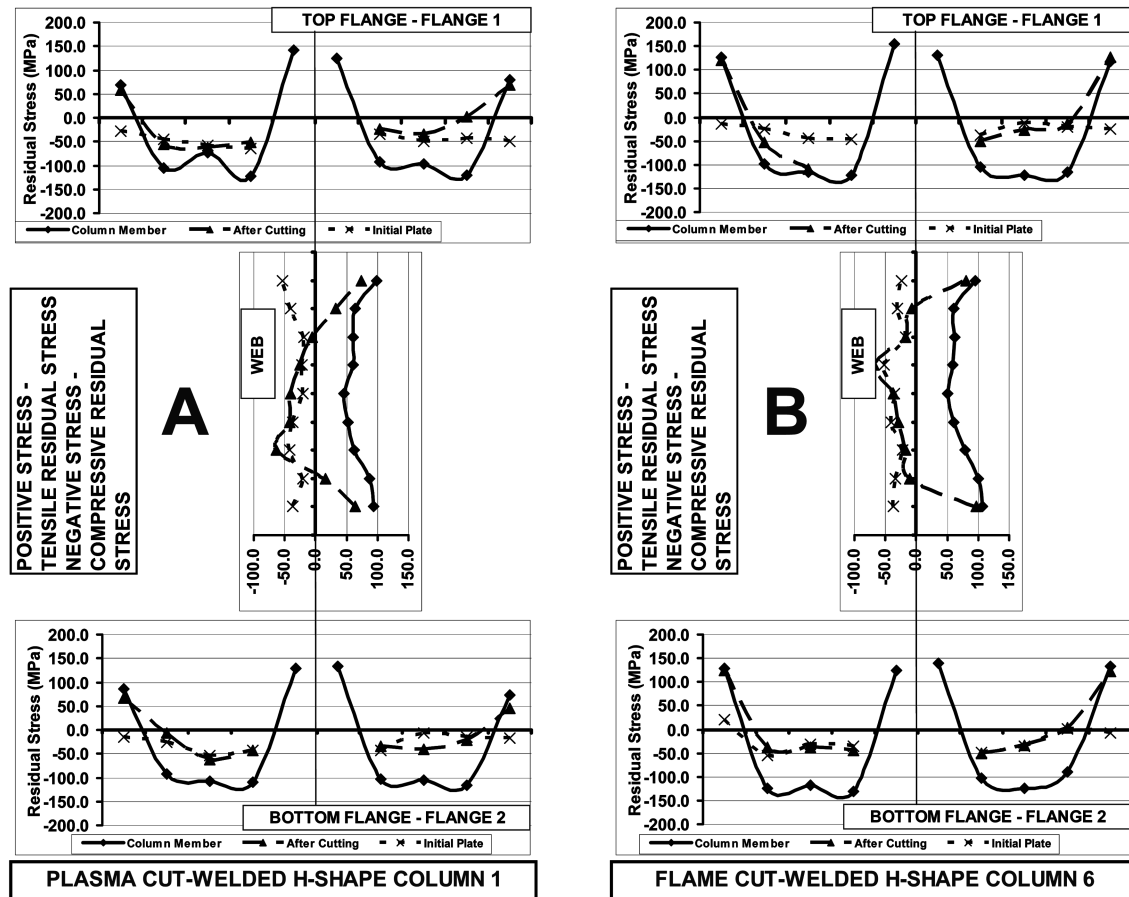
Fig. 9 Typical residual stress distributions in (a) initial plate, plasma cut plate strips, and plasma cut-welded column member, (b) initial plate, flame cut plate strips, and flame cut-welded column member

through the plate thickness (9.5 mm), so that the strain readings can be taken on either face of the steel plate. Averages of the residual stresses measured on opposite faces are given as the residual stresses presented in this paper.

As presented in Table 1, extensometer strain readings were taken at different stages of fabrication. First set of readings was taken on the large plate prior to cutting. Second set of readings was taken on the plate strips immediately after cutting. Third set of readings was taken on the long H-shaped column member (stage 3) after welding of the flange and the web plates. Fourth and the final set of readings was taken on the slices after complete sectioning by water-jet cutting. Since complete sectioning relieves the entrapped residual stress, set of readings taken on the slices becomes the initial reading corresponding to zero residual stress. Thus, in those parts of the section where the material responded in the elastic range (away from the welds), the residual strains associated with a fabrication stages can be established by finding the difference in values between initial readings and corresponding set of other measurements.

Representative residual stress patterns on plasma cut-welded H-shaped column member (Column 1) are shown in Fig. 9(a), whereas the representative residual stress patterns associated with the flame cut-
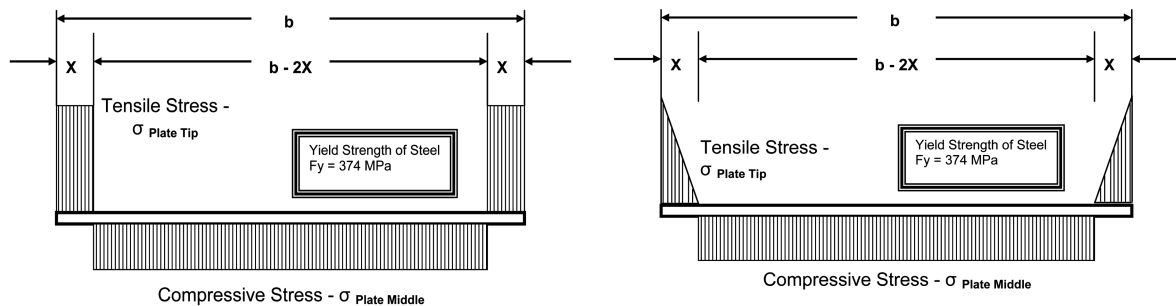
welded H-shaped column member (Column 6) are shown in Fig. 9(b). In these figures a positive stress indicates a tensile stress and a negative stress is shown as a compressive stress. The figures show the residual stresses present on the top-flange plate strip, web-plate strip, and in the bottom-flange plate strip during the following fabrication stages; initial plate, plate strip after cutting, and after welding. It is evident that the general residual stress patterns on the plate strips associated with the plasma cut-welded column members are somewhat similar to the patterns that exist on the plate strips associated with the flame cut-welded column members. As can be seen in Fig. 9, the residual stresses presented for the original plates are compressive stresses only. However, the counter balancing tensile stresses, which are not given in this figure, existed on the 100 mm and 160 mm edge remnants that were discarded (see Fig. 1). As expected, the edges of the plate strip experience tensile residual stress, whereas the middle of the plate strips experiences compressive residual stresses. The difference in stresses between the original plate and the plate strip indicates the stresses developed due to cutting operations. Similarly, the difference in stresses between a plate strip and the whole section reflects the stresses developed due to welding operations.

Based on these residual stress measurements the following general observations were made; [1] The residual stress patterns on three identically fabricated structural members are similar. [2] The cutting operation heavily influences the residual stresses closer to cutting edges, which was due to the heat input to the edges during cutting operation. [3] Tensile residual stresses exist at the flange tips, at the flange-web junctions, and at the web portions of both plasma cut-welded column members and flame cut-welded column members. Due to high heat input during the welding operation at the juncture of the flange and the web, very high tensile residual stresses exist at the web-flange intersection. [4] The measured tensile residual stresses at the flange-web junction were almost the same for the plasma cut columns and the flame cut columns, since the high heat input from welding overrides residual stresses existed after cutting operations. [5] Since the residual stress distributions in the web portion of plasma cut-welded sections and flame cut-welded sections appear to be similar, the cutting methods appear to have had little effect on the overall residual stress distributions on the web. [6] As indicated earlier, Fig. 9 shows the average residual stress on the elements established based on the surface residual stresses on opposite faces. The difference between the measured surface residual stresses on the opposite faces was relatively small at most of the locations. Thus, it can be stated that the residual stress variation through the thickness for thin plate, such as the 9.5 mm plate considered herein, is negligible.

Table 4 summarizes the residual stresses at the plate strip edges and at the plate middle, after cutting. The tensile stresses at the plate tips are based on the readings on the gauge holes adjacent to tips (about 8 mm from the edge). The compressive stresses at the plate middle are the average stress values based on three gauge-hole readings on either side of the weld. The gauge-hole readings from weld locations and the reading from the web are not used to establish the residual stresses on plate strips after cutting, since those parts of the section responded inelastically during welding. Based on Table 4, the plasma cut plates experience a tensile stress of about 61 MPa at the edges and an average compressive stress of about 35 MPa in the mid-regions whereas, the flame cut plates experience a tensile stress of about 128 MPa at the edges and an average compressive stress of about 28 MPa in the mid-regions. Two models for idealized residual stress distributions for a plasma cut plate and for a flame cut plate have been proposed in Fig. 10. In model 1, the residual stress distribution consists of equal uniform tensile zones at the edges and a balancing uniform compressive zone in the middle. In this model, plasma cut plates experience a tension of 0.163 Fy for 18% of the plate width on either edge, whereas the flame cut plates experience a tension of 0.342 Fy for 9% of the plate width on either edge, where Fy is the yield strength of the plate. In model 2, the residual stress distribution consists of triangular tensile zones at the edges

Table 4 Residual stress on the flange tip and at the flange middle of plasma cut and flame cut plates

	Plasma cut plate strips			Flame cut plate strips		
Location	Plate 1	Plate 3	Plate 5	Plate 2	Plate 4	Plate 6
Top Flange – Left Tip	+57.6 MPa	+79.6 MPa	+79.2 MPa	+136.6 MPa	+137.6 MPa	+120.0 MPa
Top Flange – Right Tip	+69.5 MPa	+68.5 MPa	+56.4 MPa	+121.6 MPa	+123.2 MPa	+126.3 MPa
Bottom Flange – Left Tip	+67.7 MPa	+58.8 MPa	+50.5 MPa	+154.3 MPa	+115.1 MPa	+123.6 MPa
Bottom Flange – Right Tip	+44.8 MPa	+52.3 MPa	+44.4 MPa	+131.7 MPa	+120.2 MPa	+121.8 MPa
Flange Tip (Average)	+59.9 MPa	+64.8 MPa	+57.6 MPa	+136.0 MPa	+124.0 MPa	+122.9 MPa
$\sigma_{Plate\ Tip}$	+61 MPa			+128 MPa		
Top Flange – Left Middle	-56.6 MPa	-38.0 MPa	-41.5 MPa	-24.1 MPa	-22.8 MPa	-46.1 MPa
Top Flange – Right Middle	-18.4 MPa	-27.6 MPa	-15.9 MPa	-0.9 MPa	-9.3 MPa	-30.6 MPa
Bottom Flange – Left Middle	-36.5 MPa	-36.0 MPa	-34.3 MPa	-47.5 MPa	-38.4 MPa	-39.9 MPa
Bottom Flange – Right Middle	-32.1 MPa	-46.8 MPa	-34.2 MPa	-24.0 MPa	-22.9 MPa	-27.3 MPa
Flange Middle (Average)	-35.9 MPa	-37.1 MPa	-31.5 MPa	-24.1 MPa	-23.3 MPa	-36.0 MPa
$\sigma_{Plate\ Middle}$	- 35 MPa			-28 MPa		

(a) MODEL 1

	PLASMA CUT PLATES	FLAME CUT PLATES
Tensile Stress – $\sigma_{Plate\ Tip}$	0.163 Fy (+61 MPa)	0.342 Fy (+128 MPa)
Compressive Stress – $\sigma_{Plate\ Middle}$	0.094 Fy (-35 MPa)	0.075 Fy (-28 MPa)
Tensile Zone – (x/b)	**0.183**	**0.090**

(b) MODEL 2

	PLASMA CUT PLATES	FLAME CUT PLATES
Tensile Stress – $\sigma_{Plate\ Tip}$	0.326 Fy (+122 MPa)	0.684 Fy (+256 MPa)
Compressive Stress – $\sigma_{Plate\ Middle}$	0.094 Fy (-35 MPa)	0.075 Fy (-28 MPa)
Tensile Zone – (x/b)	**0.183**	**0.090**

Fig. 10 Idealized residual stress distributions for a plasma cut plate and for a flame cut plate (a) Model 1, (b) Model 2

and a balancing uniform compressive zone in the middle. However, the tensile stress at the plate tip is taken to be double that of the residual stress measured at the gauge hole location near the tip, which was about 8 mm from the edge of the plate. According to this proposed model, plasma cut plates experience a plate tip tension of 0.326 Fy with a triangular reduction in stress for 18% of the plate width, whereas the flame cut plates experience a plate tip tension of 0.684 Fy with a triangular reduction in stress for 9% of the plate width.

Table 5 Residual stress on the plasma cut-welded H-shape and flame cut-welded H-shape column members

	Plasma cut welded H-shape			Flame cut welded H-shape		
Location	Column Member 1	Column Member 3	Column Member 5	Column Member 2	Column Member 4	Column Member 6
Top Flange – Left Tip	+68.1 MPa	+79.4 MPa	+98.4 MPa	+148.3 MPa	+139.0 MPa	+126.0 MPa
Top Flange – Right Tip	+79.6 MPa	+74.3 MPa	+76.6 MPa	+130.3 MPa	+134.3 MPa	+117.2 MPa
Bottom Flange – Left Tip	+85.4 MPa	+62.6 MPa	+71.7 MPa	+168.1 MPa	+129.3 MPa	+127.7 MPa
Bottom Flange – Right Tip	+73.1 MPa	+81.4 MPa	+65.4 MPa	+145.8 MPa	+121.2 MPa	+131.9 MPa
Flange Tip (Average)	+76.6 MPa	+74.4 MPa	+78.0 MPa	+148.1 MPa	+130.9 MPa	+125.7 MPa
$\sigma_{Flange\ Tip}$	+ 76 MPa			+ 135 MPa		
Top Flange – Left Middle	-99.7 MPa	-108.3 MPa	-109.7 MPa	-109.8 MPa	-122.5 MPa	-112.5 MPa
Top Flange – Right Middle	-104.0 MPa	-92.4 MPa	-54.1 MPa	-110.4 MPa	-114.7 MPa	-114.1 MPa
Bottom Flange – Left Middle	-103.8 MPa	-98.1 MPa	-97.4 MPa	-115.7 MPa	-117.8 MPa	-124.4 MPa
Bottom Flange – Right Middle	-107.9 MPa	-96.3 MPa	-99.5 MPa	-121.7 MPa	-99.1 MPa	-105.8 MPa
Flange Middle (Average)	-103.8 MPa	-98.8 MPa	-90.2 MPa	-114.4 MPa	-113.5 MPa	-114.2 MPa
$\sigma_{Flange\ Middle}$	-98 MPa			-114 MPa		
Web Middle	+62.0 MPa	+72.9 MPa	+52.1 MPa	+58.5 MPa	+56.7 MPa	+67.5 MPa
$\sigma_{Web\ Middle}$	+ 62 MPa			+ 61 MPa		

   Similarly, Table 5 shows the tensile and compressive residual stresses at flange tips, flange middle and the web-middle. The residual stress values given for the flange tip are the tensile stresses measured at the last gauge-hole. However, the stresses associated with the flange-middle and web-middle are based on the average of the residual stresses measured in these regions. Accordingly, the residual stresses on the plasma cut-welded H-shaped column member can be taken as; flange-tip +76 MPa, flange-middle -98 MPa, and web-middle +62 MPa. Similarly, the residual stresses on a flame cut-welded H-shaped column member may be taken as; flange-tip +135 MPa, flange-middle -114 MPa, and web-middle +61 MPa. From this analysis, it may be stated that the plasma cut–welded H-shaped columns experience considerably lesser residual stresses. Once again, two models have been proposed for residual stresses in H-shaped columns fabricated from plasma cut plates. Assuming uniform residual stresses in the flange tip and in the middle regions of the flange and the web, and assuming uniform stress of magnitude equalling to yield stress at the web-flange intersection, idealized residual stress distributions for a plasma cut-welded column member, and for a flame cut-welded column member have been proposed in Fig. 11(a). Based on the observations on the experimental residual stress patterns (see Fig. 9), it was further assumed that the tension zone widths at the flange tips and at the web-flange junction are equal. Accordingly, a plasma cut-welded column member contains tensile residual stresses of Fy at the web-flange welded zone, and it contains tensile residual stresses of magnitude 0.203 Fy at the flange edges. Both these zones stretch to about 4% of the flange width. Compressive residual stresses of 0.262 Fy exist at the remaining flange zones. Similarly, it has been postulated that a flame cut-welded column member contains tensile residual stresses of magnitude 0.361 Fy at the flange tip in addition to Fy at the web-flange junction. Both these zones stretch to about 5% of the flange width. Compressive residual stresses of 0.305 Fy exist at the remaining flange zones. Fig. 11(b) shows the proposed model 2, which is different from Model 1 in two aspects, the tension zones at the flange edges and at the flange-web junctions are assumed to be linearly varying, and the peak tension at the flange edge is assumed to be double that of the residual stress measured at the gauge
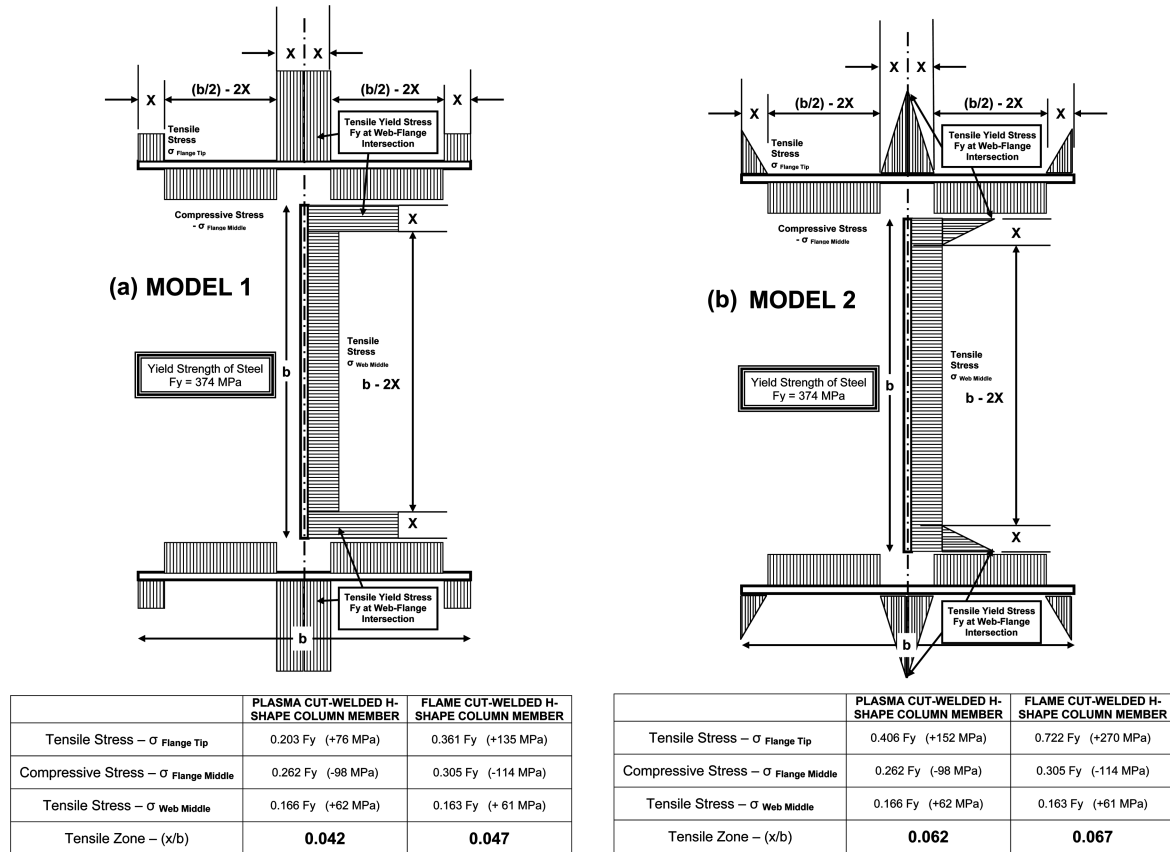
Fig. 11 Idealized residual stress distributions for a plasma cut-welded H-shape column member and for a flame cut-welded H-shape column member (a) Model 1, (b) Model 2

hole location near the tip, which was about 8 mm from the edge of the plate. Based on this model, a plasma cut-welded column member contains tensile residual stresses of magnitude 0.406 Fy at the flange edges. Both the tension zones at the web-flange junction and at the flange edges stretch to about 6% of the flange width. Similar calculations for a flame cut-welded column member result in tensile residual stresses of magnitude 0.722 Fy at the flange tip in addition to Fy at the web-flange junction. Both these zones stretch to about 7% of the flange width. Compressive residual stresses of 0.305 Fy exist at the remaining flange zones.

6. Conclusions

An experimental investigation was conducted to establish the geometric imperfections and the built-in residual stresses present in plasma cut-welded H-shaped steel column members and in similar flame cut-welded H-shaped steel columns. It is also of interest to measure the temperature profiles associated with these fabrication methods, which may be used in the verification of analytical models. The temperature measurements were taken during and after the cutting process, as well as during and after

the welding process. The typical striking temperature measured during plasma cutting was about 650°C, whereas the typical striking temperature measured during flame cutting was about 850°C. The maximum temperature measured in the plate immediately after plasma cutting was 34°C, whereas the maximum temperature after flame cutting was 127°C. A maximum temperature of 240°C was measured immediately after the welding process in each column section. The temperature at flange-web junction was observed to be the highest temperature. A maximum temperature of 200°C was noted at one of the flange tips.

The geometrical imperfections in this investigation, such as sweep and camber, were established at various stages of the fabrication processes, such as [a] the original plates, [b] the plate strips after cutting, and [c] the column sections to be tested. The sectional variations such as out-of-squareness of the section and out-of-flatness of sectional elements were also observed for each column section. The largest out-of–plane imperfections for the whole plate, plate strip, and the H-shaped columns were (L/305), (L/233), and (L/685), respectively, where L is the length of the corresponding member. Geometric imperfections associated with plasma cut element and members are less than those of the corresponding elements and members made by flame cutting. The variations in the sectional dimensions were well within the permissible values given in the current steel design standards, though the cross-sections of column members 2, 4 and 6, which were fabricated from flame-cut plate strips, exhibited larger out of parallel and out of squareness.

The "Method of Section" technique, where a 305 mm long piece of the H-section was sliced into 15 mm thin slices, was used to establish the residual stresses in the plate, plate strip, and in the welded columns. The residual stress variation through the thickness was observed to be relatively small. Plasma cut plates experience a tensile stress of about 61 MPa at the edges and an average compressive stress of about 35 MPa in the mid-regions whereas, the flame cut plates experience a tensile stress of about 128 MPa at the edges and an average compressive stress of about 28 MPa in the mid-regions. Based on the test results the residual stresses on the plasma cut-welded H-shaped column member can be taken as; flange-tip +76 MPa, flange-middle -98 MPa, and web-middle +62 MPa. Similarly, the residual stresses on a flame cut-welded H-shaped column member may be taken as; flange-tip +135 MPa, flange-middle -114 MPa, and web-middle +61 MPa. Further, the shape of the distribution of residual stresses is somewhat similar for plasma-cut and for flame-cut sections. Based on these observations, two models for idealized residual stress distributions for a plasma-cut plate and a flame cut plate and two models for plasma cut-welded column member and for flame cut-welded columns have been proposed.

Acknowledgements

References

Arasaratnam, P. (2005), "Characteristics and behaviour of plasma cut-welded H-shaped steel columns", M.A.Sc. Thesis, Department of Civil Engineering, McMaster University, Hamilton, Ontario, Canada. L8S 4L7, p.xiii, 7-11.

ASTM Standards (2004), Standard Specification for General Requirements for Rolled Structural Steel Bars, Plates, Shapes, and Sheet Piling, Document Number: ASTM A6/A6M-04, American Society for Testing and Materials, Philadelphia, U.S.A.

CISC (2004), Handbook of Steel Construction, Canadian Institute of Steel Construction, Willowadale, Ontario, Canada.

CSA (2001), CAN/CSA-S16-01 Limit States Design of Steel Structures, Canadian Standards Association, Mississauga, Ontario, Canada.

Fukumoto, Y. and Itoh, Y. (1983), "Evaluation of multiple column curves using the experimental data-base approach", *J. Const. Steel Res.*, **3**(3), 1-18.

Galambos, T. V. (1988), *Guide to Stability Design Criteria for Metal Structures-B.6 Technical Memorandum No.6: Determination of Residual Stresses*, 4th Edition, John Wiley & Sons, New York, U.S.A., 734-744.

Huber, A. W. and Beedle, L. S., (1954), "Residual stress and the compressive strength of steel", *Welding Journal*, Research Supplement, **33**, December, pp. 589-s-614-s.

Kandil, F. A., Lord, J. D., Fry, T. A. and Grant, P. V., (2001), A Review of Residual Stress Measurement Methods – A Guide to Technique Selection.

Lindgren, L. E. (2001a), "Finite element modelling and simulation of welding. Part 1: Increased complexity", *J. Thermal Stresses*, **24**(2), 141-192.

Lindgren, L. E. (2001b), "Finite element modelling and simulation of welding. Part 2: Improved material modelling", *J. Thermal Stresses*, **24**(3), 195-231.

Lindgren, L. E. (2001c), "Finite element modelling and simulation of welding. Part 3: Efficiency and integration", *J. Thermal Stresses*, **24**(4), 305-334.

Nagaraja Rao, N. R. and Tall, L. (1961), "Residual stresses in welded plates", *Welding Journal*, Research Supplement, **40**, October, pp. 468-s-480-s.

Potdar, Y. K. and Zehnder, A. T. (2003), "Measurement and simulation of temperature and deformation fields in transient metal cutting", *J. Manuf. Sci. Eng.*, **125**, 645-655.

SA (1998), Steel Structures – AS4100-1998, Standards Association of Australia, Homebush, NSW 2140, Australia.

BU